Microelectronic Engineering 97 (2012) 204–207

Contents lists available at SciVerse ScienceDirect

Microelectronic Engineering

journal homepage: www.elsevier.com/locate/mee

Optimization of surface plasmon polariton generation in a nanocone through linearly polarized laser beams

M. Malerba [a], A. Alabastri [a], G. Cojoc [b], M. Francardi [b], M. Perrone Donnorso [a], R. Proietti Zaccaria [a], F. De Angelis [a,b,*], E. Di Fabrizio [a,b]

[a] *Fondazione Istituto Italiano di Tecnologia, IIT, Via Morego 30, 16163 Genova, Italy*
[b] *Università della Magna Graecia di Catanzaro, Dipartimento di Medicina, Viale Europa, 88100 Catanzaro, Italy*

ARTICLE INFO

Article history:
Available online 19 March 2012

Keywords:
Plasmonics
Photonics
TERS
SPP
Surface plasmon polariton
Raman
Linear polarization

ABSTRACT

In this paper we present numerical FDTD calculations, optimizing experimental setup conditions for surface plasmon polariton (SPP) generation. The simulation considers a silver nanocone placed on a Si_3N_4 membrane, and studies the effects on the apex for a linearly polarized Gaussian light beam impinging from below or from the side of the cone. Radially polarized focused beams already proved to generate efficiently SPPs; in this work, we show that also linear polarization leads to an efficient generation of SPPs on the cone surface, as long as tilt angle and numeric aperture are optimized. In particular, we show that our setup conditions and proposed device, designed for a $\lambda = 633$ nm linearly polarized He–Ne laser, can enhance the incoming electric field up to 150 times at the apex of the cone.

1. Introduction

Plasmonic structures, when scaled down to few tens of nanometers, have been identified as very good candidates for detection of organic compounds and biochemical characterization, even with a sensitivity down to single molecule [1–4].

On one hand, overcoming the limits of SERS substrates, researchers have developed many different approaches which span from microfluidic and hydrophobic systems [5–7] to advanced nanofabrication devices [8–10] including specific metallic structures, able to produce hot spots [11–18] *i.e.* localized high intensity electric fields. Although this approach can give very high signals and employs well established lithographic techniques, it is affected by randomness when it comes to selecting specific areas or features of the analyzed specimen. Grated metallic tips [19–21] have been also used by shining light directly on the apex, obtaining high intensity local fields and the possibility of selecting the zone of interest within the sample to characterize. Such nanostructures however need to be excited directly on the tip, giving a detected signal which is affected by a poor signal to noise ratio, and a lower efficiency.

On the other hand, more recently, tapered surface plasmon waveguides have caught the attention of researchers, showing an adiabatic behaviour and a superfocusing effect of optical energy [22,23]. Theoretical calculations have shown a very high field in proximity of the apex, as shown for example in [24]. In particular, when spatial decoupling of the source from the emitted signal is employed [25,26], the signal-to-noise ratio is improved but it becomes crucial to obtain high coupling efficiencies between source and device. Structures such as metallic nanocones grown on specially tailored photonic crystals have shown interesting results, high optical fields and good resolution, thus allowing chemical mapping of both organic and inorganic systems with a resolution comparable to that of AFM [25–27].

Regarding the maximization of the coupling efficiency (high electric field at the tip apex), a radial polarization in principle gives best results, but has been suggested to present some difficulties in terms of alignment and focusing [28]. We show instead that also a linear polarization can lead to high intensity fields, but some specific geometry is needed to locally generate a *TM0-like* mode that mimics the behaviour of radial polarizarion [27]. One of these is the tilting of the beam with respect to the cone axis. We have therefore performed numeric simulations to optimize two experimental tuneable parameters: angle of incidence and beam numeric aperture. We conclude that under certain conditions, intense electric fields can be obtained at the apex of the cone, thus simplifying the setup and the experiment.

* Corresponding author at: Fondazione Istituto Italiano di Tecnologia, IIT, Via Morego 30, 16163 Genova, Italy. Tel.: +39 010 71781249.
E-mail address: francesco.deangelis@iit.it (F. De Angelis).

0167-9317/$ - see front matter © 2012 Elsevier B.V. All rights reserved.
http://dx.doi.org/10.1016/j.mee.2012.02.026

2. Simulation setup

This calculation was carried out using *Lumerical FDTD Solutions* software.

The simulated object is as much as possible resembling a structure built with current state-of-the-art bottom-up nanofabrication limits. It consists of a silver nanocone with a 300 nm diameter base, a height of 1.7 μm and a rounded apex with a radius of 5 nm, laying on a perfect dielectric ($n = 2$) 160 nm thick substrate.

The simulation was run within two different configurations (Fig. 1). In the bottom configuration the electromagnetic wave is injected from below. The source is placed 0.2 μm below the dielectric slab, and is modelled as a Gaussian field distribution with increasing numeric apertures (NAs), in three different cases: $NA = 0.1$ (mimicking a plane wave), $NA = 0.5$ and $NA = 0.7$. The lateral size of the Gaussian beam distribution for $NA = 0.5$ and $NA = 0.7$ is respectively 800 nm and 500 nm, considering the diameter of the spot down to where the intensity drops to 50% of the maximum (spot size is roughly given by $\lambda/2{*}NA$). In each case the injection angle is varied from 0 to 60 degrees with 5 degrees steps. The cone-source distance is kept constant whereas the lateral coordinates of the source are varied to let the laser beam impinge on the edge of the nanocone base.

The lateral configuration takes into account same NAs and tilt angles, but is orthogonal to the former one: the Gaussian beam is generated at a distance of 0.5 μm from the come, and impinges from the side. Again, the point of injection is kept constant, and is placed at a height of 300 nm from the base of the cone.

Simulation mesh size was set to give a high computing resolution near to the region of interest, i.e. the apex of the cone. Mesh elements (cubes) in the bottom region, containing source and dielectric, have a side of 20 nm; elements contained in the central part of the cone measure a side of 5 nm, while the apex, for a length of 50 nm, is set to have a meshing resolution of 1 nm. The entire FDTD simulation region is a 2 μm × 1 μm × 2.7 μm parallelepiped. Boundary conditions were chosen to be PML, guaranteeing no reflection on the boundaries.

The source wavelength was set to cover the range between 530 and 1030 nm, thus simulating part of the visible and IR spectrum, while the amplitude of the EM field is equal to 1 V/m. All results must therefore be compared to such source values.

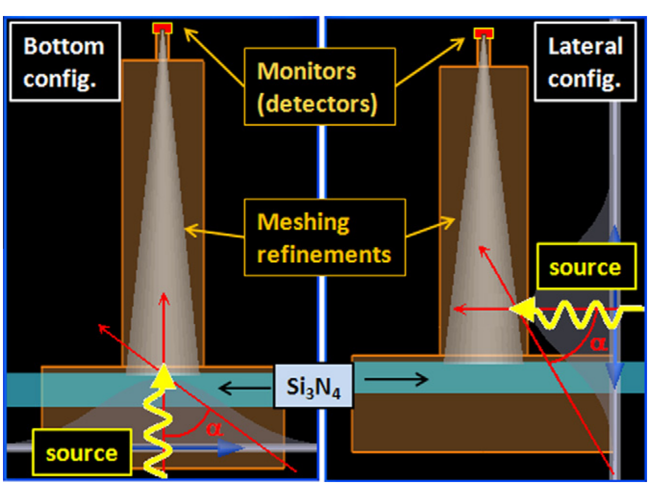

Fig. 1. Simulation setup: light is injected from below or from the side, and its angle is varied as shown. In the bottom configuration, zero degrees injection angle describes a wave direction parallel to the cone's axis, and increases with a counter-clockwise tilt. In the lateral configuration the zero degrees angle propagation is perpendicular to the axis, and increases with a clockwise tilt. Orange rectangles represent three different meshing regions. For interpretation of the references to colour in this figure legend, the reader is referred to the web version of this article).

3. Results and discussion

For each simulation, the monitor recording the data is a 50 nm by 50 nm square, centred at the apex. The source spectrum is discretized in a finite number of wavelengths, with a step of $\Delta\lambda = 10$ nm. For each wavelength and each tilt angle, the maximum electric field value recorded anywhere inside the monitor is saved and then plotted; the result is a 2D intensity colour plot with angle of incidence and wavelength as independent variables (Figs. 2 and 4).

Fig. 2a–c, depicting results for an illumination impinging from below, show that maximum intensity is dependent on wavelength and tilt angle. In particular, local maxima are found at wavelengths $\lambda = 580, 630, 710, 830, 995$ nm independently of the chosen NA and tilting angle. We notice that these values depend on the cone geometry (height, vertex angle, and base width) and they slightly change when different geometries are considered. For the simulated geometry, absolute maxima are obtained when using a numeric aperture of 0.5, and when tilting the source between 30 and 40 degrees. It can be seen that in such configuration, at the typical wavelength of a He-Ne laser ($\lambda = 633$ nm), the electric field on the tip apex reaches the value of 150 V/m which corresponds to a field enhancement equal to 150.

A preliminary comparison of the first three images suggests a solid shift of all maxima along the angle axis when changing numeric aperture, spanning from 20 degrees ($NA = 0.1$) to 40 degrees ($NA = 0.7$), but it does not show a change along the wavelength axis. We notice that the SPP generation occurs at the edge of the nanocone base since the edge can provide the necessary momentum. The reason why a certain NA is more efficient than other is not clear and further investigations are required. Under a qualitative point of view, we point out that from one hand higher NA objectives produce smaller beam spots, enabling a more efficient light delivery on the nanocone base. Therefore, they should be more efficient with respect to lower NA ones. On the other hand, high NA lenses induce stronger polarization distortion (the z-component of the electric field increases) that could result in a lower coupling efficiency.

Our analysis also shows a non-linear trend in the distribution of maxima and minima as a function of wavelength. As mentioned above, it depends on the cone geometry: the base width affects the coupling with the incoming wavelength, the vertex angle affects the variation of index of refraction along the nanocone (adiabatic compression [22,23]), and the tip size determines whether the adiabatic compression is relevant (no reflection on the tip) or not (tip reflects backwards). The overall effect looks as the one occurring in a plasmonic resonant antenna, and relies on standing waves formation [28,29]. In Fig. 3 is reported the electric field distribution along the nanocone for different wavelengths. SPP waves running toward the tip are visible. The scale is logarithmic, in order to appreciate the lower intensities of the waves far from the apex. The different electric field intensities at the tip ends between the considered wavelengths is not appreciable on this scale.

Fig. 4 depicts results for the second geometry (lateral configuration). The analysis of these results is more difficult due to the particular geometrical and optical configuration: in fact, as we sketched in fig. 1, the source laser beam in part directly impinges on the nanocone, in part is refracted when it penetrates into the dielectric (undergoing a phase shift) and finally impinges on the nanocone.

The result is a "dirty source" that impinges on the base of the nanocone. Therefore, it is not clear which of these components enables an efficient laser/nanocone coupling. We could run simula-